COMPUTER METHODS AND PROGRAMS IN BIOMEDICINE 104 (2011) 480–488

journal homepage: www.intl.elsevierhealth.com/journals/cmpb

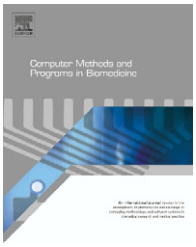

Wavelet-based de-noising techniques in MRI

Karel Bartušek[a,*], *Jiří Přinosil*[b], *Zdeněk Smékal*[b]

[a] *Institute of Scientific Instruments, Academy of Sciences, Czech Republic*
[b] *Brno University of Technology, Czech Republic*

ARTICLE INFO

Article history:
Received 15 April 2010
Received in revised form
20 July 2011
Accepted 29 August 2011

Keywords:
Wavelet transformation
Filtering technique
Magnetic resonance imaging

ABSTRACT

The paper deals with techniques for the enhancement of magnetic resonance (MR) images using the wavelet analysis, which is assessed from the viewpoint of choosing the mother wavelet and the thresholding technique. Three parameters are used as objective criteria of the quality of image enhancement: the signal-to-noise ratio (SNR), image contrast, and linear approximation of edge steepness. Unlike most of the standard methods, which work exclusively with image magnitude, we also examined the influence of image phase, i.e. the image is processed as a complex signal. In addition to the interpretation of results, a short summary is given that deals with the choice of the optimal mother wavelet and thresholding technique for different types of MR images.

1. Introduction

The time of MRI (Magnetic Resonance Imaging) is limited by patients' comfort, non-stabilities and artifacts of the tomography system, and physical limits during dynamical applications such as heart imaging or functional MRI. At present, fast methods of magnetic resonance (EPI) are used, which allows significant reductions of investigation time. Retrieved images have a low signal-to-noise ratio (SNR) and a small contrast. In MR imaging microscopy or for very thin slices of plants it is possible to use the time averaging of signal for SNR improvement, which has no effect on spatial resolution in the image. Extending the measurement time is acceptable for such objects. But this is not feasible in medicine and therefore a post-process image filtering (image de-noising) has to be used for SNR improvement. The drawback of any digital image filtering technique is the reduction in sharpness, resolution, and image contrast.

It is well known that magnitude image data of magnetic resonance obey the Rician distribution. Unlike additive Gaussian noise, Rician "noise" is signal-dependent, and separating signal from noise is a difficult task. Rician noise is especially problematic in low SNR regimes, where it not only causes random fluctuations but also introduces a signal-dependent bias into the data, which reduces image contrast.

The application of wavelets for the de-noising of MR images has been pioneered by Weaver et al. [1], who applied their de-noising scheme to MR images of the human neck. They concluded that the de-noising scheme can reduce noise by 10%–50% without reducing edge sharpness.

De-noising techniques operating with magnitude images have been proposed in most cases only for disease diagnostic from MR images with a low SNR. Henkelman [2] shows the relationship between the true signal amplitude and that which is measured in real and magnitude images in the presence of noise. Correction factors for actual experimental measurements are demonstrated. Some recent work by Nowak [3] employs a wavelet-based method for de-noising the square magnitude images, and explicitly takes into account the Rician nature of the noise distribution.

A few works have been devoted to phase image de-noising, despite the existence of important applications like current density imaging (CDI), MRI and functional MRI. Alexander [4]

* *Corresponding author*. Tel.: +420 541514341; fax: +420 541514402.
E-mail address: bar@isibrno.cz (K. Bartušek).
0169-2607/$ – see front matter © 2011 Elsevier Ireland Ltd. All rights reserved.
doi:10.1016/j.cmpb.2011.08.008

applies a wavelet de-noising algorithm directly to the complex image obtained as the Fourier transform of the raw *k*-space two-channel (real and imaginary) data. By retaining the complex image, he is able to de-noise not only magnitude images but also phase images. A multi-scale (complex) wavelet-domain Wiener-type filter is derived. The algorithm preserves the edges when the Haar wavelet rather than smoother wavelets, such as those of Daubechies, are used. Zaroubi [5] presents a fast post-processing method for noise reduction of MR images, termed complex de-noising. The method is based on shrinking noisy discrete wavelet transform coefficients via thresholding, and it can be used for any MRI data-set with no need for high power computers. The de-noising algorithm is applied to the two orthogonal sets of complex MR images separately. Cruz-Enriquez [6] applies a group of de-noising algorithms in the wavelet domain to the complex image, in order to recover the phase information. Significant improvements in SNR for low initial values are achieved by using the proposed filters.

2. Materials and methods

2.1. SNR, contrast and slope edge estimates

For phantom MRI images with different SNR, the improvement of the SNR, contrast and linear slope edge approximation are measured before and after the application of de-noising algorithm. The SNR and contrast are computed in two regions of interest in each image: the first region contains only noisy background, while the second region contains, in addition, the signal. We use the definition of parameters according to Eqs. (1) and (4). The linear slope edge approximation is estimated over a selected sharp edge in the MRI image.

The SNR in an MR image is computed as the squared mean intensity of the selected area relative to the underlying Gaussian noise variance $\sigma_N{}^2$. The SNR of the image magnitude is defined as [3]:

$$\mathrm{SNR} = 10\log_{10}\left(\frac{I_{\mathrm{mean}}^2}{\sigma_{\mathrm{N}}^2}\right), \tag{1}$$

where I_{mean} is obtained as the mean value of intensity I in a homogenous region-of-interest (ROI) inside the image (signal), and σ_N is the standard deviation of the ROI without signal (background). If we take into consideration the averaging of the number of MR acquisitions N_{acq}, the standard deviation of noise is equal to:

$$\sigma_{\mathrm{eff}} = \frac{\sigma_{\mathrm{N}}}{\sqrt{N_{\mathrm{acq}}}}. \tag{2}$$

The contrast of image intensity I is defined as:

$$C_{AB} = |I_A - I_B|. \tag{3}$$

The relative contrast is defined as a contrast which is related to reference image intensity I_{ref} ($I_{\mathrm{ref}} = (I_A + I_B)/2$):

$$C_{\mathrm{rel}} = \left(\frac{C_{AB}}{I_{\mathrm{ref}}}\right) = 2\frac{|I_A - I_B|}{I_A + I_B}, \tag{4}$$

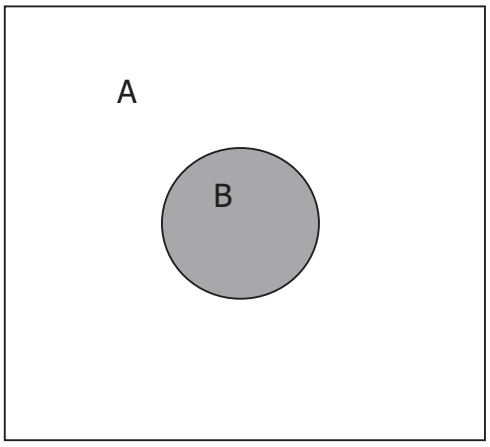

Fig. 1 – MR image of the phantom for the contrast definition.

where I_A and I_B are the mean image intensities of A and B image areas, as shown in Fig. 1.

The linear slope edge approximation m can be estimated using Eq. (5) applied to a selected sharp edge, which is represented as 1D signal. Due to the presence of noise in the MR image, the measurement is realized on several places of the edge and the median of measurements is computed:

$$m = \frac{\Delta y}{\Delta x}, \tag{5}$$

where Δy and Δx represent the gradients of image intensity and scale, respectively, as shown in Fig. 2.

2.2. De-noising algorithms

As already mentioned above, we utilize a wavelet-based algorithm for MR image noise reduction. The wavelet transform WT is an integral transform for the "time–frequency" description of the signal being analyzed. It can be used in various signal processing applications, e.g. signal compression, feature extraction, and noise removal. In our case, we use the

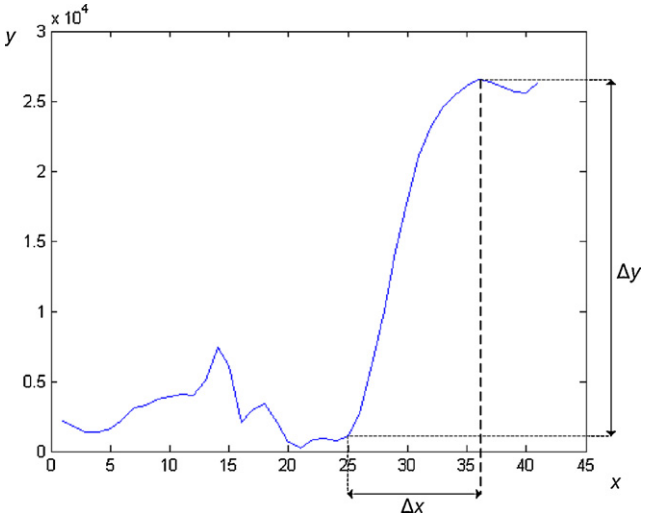

Fig. 2 – Example of the linear slope edge estimation.

two-dimensional dyadic discrete-time wavelet transform 2D-DTWT, which uses mother wavelet function φ to decompose a digital image into a multilevel set of approximations: vertical, horizontal and diagonal wavelet coefficients c^l, c^l, c^l and c^l, where $l = 1, 2, \ldots, L$ gives the level of decomposition. A more detailed description of the wavelet transform and its properties can be found, for example, in [7].

The most frequently used technique for MR image noise reduction using the wavelet coefficients is thresholding. It is assumed that the wavelet coefficients with values lower than a particular threshold value T corresponds to noisy samples and they can be therefore cancelled, which leads to noise reduction in the image domain. When the remaining coefficients are unaffected, it is called hard thresholding:

$$\hat{c}(x, y) = \begin{cases} c(x, y) & \left|c(x, y)\right| \geq T \\ 0 & \left|c(x, y)\right| < T \end{cases}. \tag{6}$$

Another often used kind of thresholding technique is the so-called soft thresholding, defined as:

$$\hat{c}(x, y) = \begin{cases} \text{sign}\left[c(x, y)\right]\left[\left|c(x, y)\right| - T\right] & \left|c(x, y)\right| \geq T \\ 0 & \left|c(x, y)\right| < T \end{cases}. \tag{7}$$

It can be generally said that soft thresholding yields a better SNR while hard thresholding better preserves the slope edge. There are other thresholding techniques such as semi-soft, hyperbolic, non negative garrote, etc. [8].

The most important part of the de-noising algorithm is the estimation of the optimal threshold value. When the threshold value is too low, then the noise reduction is inefficient, and, on the other hand, when it is too high, then details of image information can be lost. In our work, we consider one of the most frequently used estimation algorithms, the so-called universal threshold, defined as [10]:

$$T = \sigma_{\text{est}}\sqrt{2\log(N)}, \tag{8}$$

where N is the number of input image pixels, σ_{est} represents the standard deviation of noise, which can be estimated by the Donoho and Johnstone theorem [9] as the statistical median MAD of detailed wavelet coefficients c^l, c^l, and c^l from the first decomposition level divided by the constant 0.6745 [9]. This threshold is then applied to all detailed wavelet coefficients of each decomposition level:

$$\sigma_{\text{est}} = \frac{\text{MAD}(c_D^l)}{0.6745}. \tag{9}$$

When we consider de-noising a complex MR image, we have to first separate it into the real and imaginary parts. Then we process both parts by the wavelet transform separately, we estimate the unique threshold values for each part, and then threshold the wavelet coefficients. After that we reconstruct the image domain from the thresholded wavelet coefficients and, finally, combine them to form a de-noised complex image. The noise in both parts is assumed to be independent. The type of mother wavelets and thresholding techniques can differ for both parts.

In addition to the standard de-noising technique operating with thresholding, we also implement a method described in [4] with the Wiener filter applied to the complex wavelet coefficients (composed of the wavelet coefficients from the real and imaginary image parts). The method defined in Eq. (10) can be described as a multiplication of l-th decomposition level of detailed complex wavelet coefficients $c^l(x,y)$ by the complex value of "attenuation" factor $\alpha^l(x,y)$:

$$\hat{c}^l(x, y) = \alpha^l(x, y)c^l(x, y). \tag{10}$$

According to [4], the attenuation factor for each wavelet coefficient can be evaluated using the magnitude value of the particular coefficient and the estimated standard deviation of noise σ_{est}:

$$\alpha^l(x, y) = \left[\frac{\left|c^l(x, y)\right|^2 - \sigma^2}{\left|c^l(x, y)\right|^2}\right]_+. \tag{11}$$

Negative values of the attenuation factor are zeroed, i.e. coefficients with lower values than the estimated standard deviation of noise are eliminated, which can be computed as:

$$\sigma_{\text{est}} = \sqrt{\sigma_{\text{est}(R)}^2 + \sigma_{\text{est}(I)}^2}, \tag{12}$$

where $\sigma_{\text{est}(R)}$ is the estimated standard deviation of noise from the real MR image part and $\sigma_{\text{est}(I)}$ from the imaginary MR image part, with Eq. (9) taken into consideration.

Eq. (11) is extended by introducing an optional parameter $\tau \geq 1$, which allows the removal of the lower-value coefficients. Various values of τ are suitable for different images [4]:

$$\alpha^l(x, y) = \left[\frac{\left|c^l(x, y)\right|^2 - \tau\sigma^2}{\left|c^l(x, y)\right|^2}\right]_+. \tag{13}$$

An advantage of this method is the combination of hard thresholding for high values of $\left|c^l(x, y)\right|$ ($\alpha^l(x, y) \approx 1$), which yields a small bias (better contrast and slope edge), and soft thresholding for coefficients with values close to the level of noise, which yields a small variance (better SNR).

3. Experiments and results

3.1. MRI data

For real MRI data, a set of 2D phantom MR single-slice data from the same volunteer was acquired on a 4.7T MRI scanner (Magnex magnet, MR Solution electronics and software) in ISI Brno, using the standard spin-echo sequence. The sample applied was a square container ($40 \times 40 \times 40$ mm) filled with water. Relaxation times of water were reduced by the application of nickel sulphate. The cylindrical cuvette of 20 mm diameter was filled with gel water sample, whose relaxation times are short (11 ms), and then inserted into a dish. The tested MR images with different SNR ($T_E = 20$ ms, $T_R = 500$ ms, MA = 512×512, FOV = 60×60 mm) were coronal slices of variable thickness (0.2–0.5–1–2 mm). In addition, MR

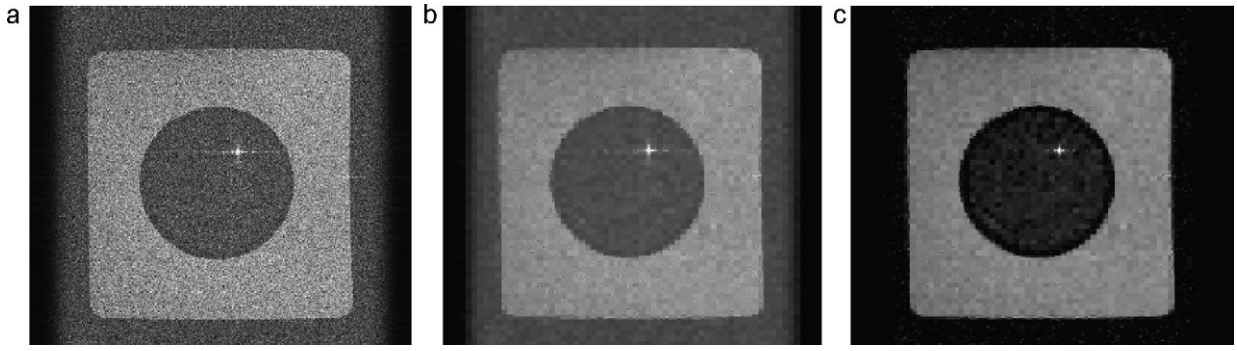

Fig. 3 – (a) Original phantom MRI with SNR = 11.4 dB, (b) magnitude image wavelet coefficients filtering with SNR = 27 dB, (c) complex image wavelet coefficient filtering with SNR = 25 dB.

images of head (with TMJ-Temporomandibular Joint) were acquired on the Philips ACHIEVA MRI system (DS = 1.5 T) in the Faculty Hospital Brno-Bohunice. The measurement parameters were: T2W-FSE pulse sequence: $T_E = 20$ ms, $T_R = 1600$ ms, MA = 256 × 256, FOV = 160 × 160 mm, sagittal slice 2 mm.

3.2. *Experiment background*

Our experiment can be divided into two parts. In the first part, the wavelet-based de-noising algorithms described above are applied to the phantom MRI, mentioned in Section 2.1. Several discrete mother wavelets (wavelet filters) are applied and the results are compared with the help of three described parameters (Section 2.1). In the experiment, we use two images with different SNR (11.4 dB and 19.1 dB) obtained by varying the slice thickness. The contrast and the linear approximation of the slope edge are related to the reference image (ratio expression) with SNR = 35 dB, because of the unreliable measurement of these parameters from noisy images. In the second part of our experiment, the same procedure is performed on the MR image of head with SNR = 33 dB, as mentioned in Section 2.1.

The choice of mother wavelets has been inspired by a paper [11] dealing with an analytical study of wavelet filters (mother wavelets) for image compression. The first change is the modification via replacing the Daubechies mother wavelet of the 7th order by the same mother wavelet of the 2nd order (more frequently used in MR de-noising) and by adding the discrete Meyer mother wavelet (often used in MR de-noising [12]). Another change consisted in applying the following mother wavelets: Haar, Daubechies 2nd and 9th orders, bi-orthogonal 2nd.2nd and 4th.4th orders, Symlet 5th order, Coiflet 5th order, and discrete Meyer. According to experiments in paper [4], the level of the wavelet decomposition is 3. The complex image wavelet coefficient filtering is only considered, because filtering the coefficients of magnitude image wavelets introduces a signal-dependent bias, as shown in Fig. 3.

3.3. *Results*

Results of de-noising the phantom MR image with SNR = 11.4 dB are given in Table 1, and given graphically in Fig. 4, where the values are normalized according to the reference value corresponding to the maximum value of a particular parameter.

The hard thresholding technique best preserves the slope edge for all wavelet filters, but it yields a lower SNR value in comparison with the soft thresholding technique. Using the Wiener filtering technique, we reach the greatest balance between the values of SNR and slope edge for all wavelet types (except for bior2.2) and, in addition, we also obtain the best contrast. Generally, the contrast value should be the highest for a thresholding technique yielding the lowest bias, i.e. hard thresholding, but in the case of a low original MR image SNR the contrast is strongly affected by the presence of noise and therefore better results can be achieved even by a technique with higher bias, i.e. soft thresholding.

The results of de-noising the phantom MR image with SNR = 19.1 dB are given in Table 2 and Fig. 5. There is a great amount of similarity with previous results excluding the contrast value, where a higher value is achieved for hard thresholding than for soft thresholding because of the better SNR of the original MR image.

While the first tested image (the MR phantom image) does not include almost any detailed information and the image could be evaluated by measuring only one significant edge, in the case of the second tested image (the MR image of head) the measurement of two various edges was applied, which differed in the magnitude of intensity change in the neighbourhood of the relevant edge (see Fig. 6). The values measured are summarized in Table 3, where m_1 defines the linear slope edge approximation with the higher intensity change, and m_2 with the lower intensity change. The resultant graphs can be seen in Fig. 7, but the contrast is not depicted here because of unimportant changes in contrast in individual thresholding techniques and the mother wavelets used.

It can be seen from Fig. 7 that the influence of thresholding itself on the resultant MR image of head approximately corresponds to the results for the MR phantom image. Therefore it is possible to say that the choice of threshold method does not depend much on the type of the image being processed. On the other hand, the results of the processed MR images are pretty dependent on the choice of the mother wavelet. It has been shown that it is advantageous to assign the mother wavelet to the chosen threshold method. The following combinations can be given as examples: hard thresholding and the

Table 1 – Results of de-noising the phantom MR image with SNR = 11.4 dB.

Wavelet filter	Hard thresholding			Soft thresholding			Wiener filtering		
	SNR	C_{rel}	m	SNR	C_{rel}	m	SNR	C_{rel}	m
haar	16.4	0.74	1.17	22.2	0.80	1.14	24.4	1.03	1.17
db2	16.3	0.75	0.50	21.3	0.81	0.41	24.6	1.02	0.52
db9	16.8	0.70	0.51	22.2	0.80	0.44	25.1	0.97	0.41
bior2.2	14.4	0.63	0.66	20.7	0.78	0.50	19.4	0.84	0.50
bior4.4	16.0	0.71	0.55	21.9	0.80	0.43	23.5	0.98	0.46
sym5	15.8	0.69	0.55	22.1	0.80	0.47	23.0	0.97	0.48
coif5	16.4	0.72	0.54	22.1	0.80	0.48	24.3	1.00	0.55
dmey	15.0	0.63	0.60	21.8	0.79	0.47	21.3	0.90	0.50

Haar wavelet, soft thresholding and the bi-orthogonal wavelet 2.2 or the Wiener filtering and the Coiflet wavelet of the 5th order. But the greatest influence on the processing of degraded image can be seen in the choice of the mother wavelet. It is evident both from the differences between the tested images (the Haar wavelet used for the MR phantom image or the bi-orthogonal wavelet 2.2 used for the MR image of head), and even from partial areas of the individual MR images. If we follow the slope ratio of two edges, m_1 and m_2, for various types of mother wavelet, we suppose that, generally, the slope edge m_2 is less than m_1. The ratio is thus high for some types of mother wavelet (the Haar wavelet, for example), but for other wavelets m_1 it can be approximately equal to m_2; m_2 can even be higher than m_1 (the discrete Meyer wavelet, for example).

4. Discussion

In this part of the paper, both an interpretation of the results obtained from experiments and a brief summary of how to

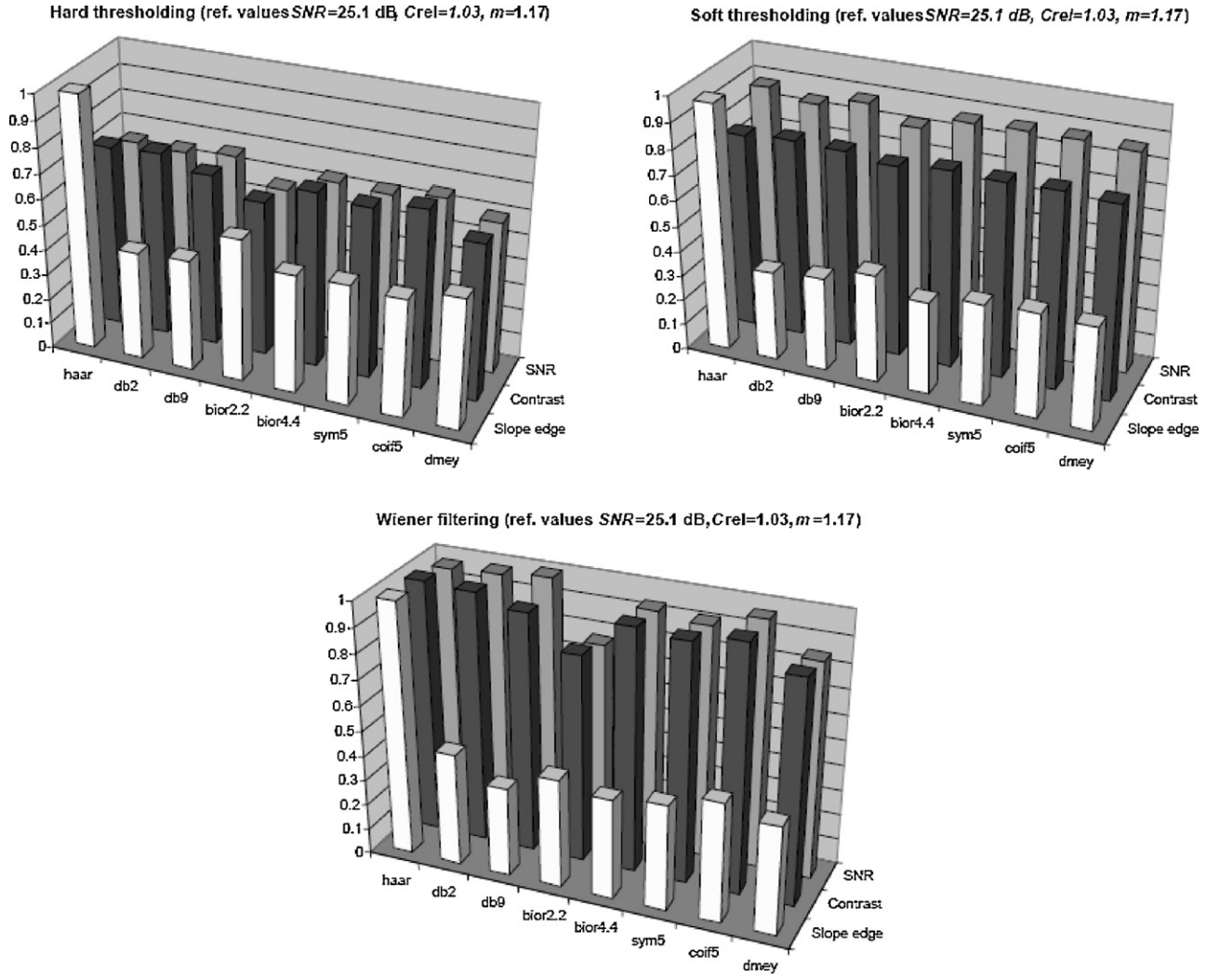

Fig. 4 – Results of de-noising the phantom MR image with SNR = 11.4 dB.

Table 2 – Results of de-noising the phantom MR image with SNR = 19.1 dB.

Wavelet filter	Hard thresholding			Soft thresholding			Wiener filtering		
	SNR	C_{rel}	m	SNR	C_{rel}	m	SNR	C_{rel}	m
haar	25.2	0.93	1.10	30.4	0.95	1.07	34.7	1.06	1.14
db2	24.7	0.93	0.85	29.6	0.96	0.61	34.1	1.05	0.70
db9	25.5	0.91	0.73	30.4	0.95	0.47	34.2	1.03	0.49
bior2.2	22.5	0.87	0.73	28.9	0.95	0.64	28.4	0.98	0.66
bior4.4	24.5	0.91	0.72	29.9	0.95	0.48	32.9	1.04	0.52
sym5	24.0	0.90	0.68	30.1	0.95	0.54	32.1	1.03	0.60
coif5	25.2	0.92	0.75	30.1	0.95	0.56	34.4	1.05	0.65
dmey	23.2	0.87	0.72	30.0	0.95	0.54	30.3	1.01	0.60

choose optimal parameters for the enhancement of different types of MR image are given.

4.1. *Interpretation of results*

Generally speaking, the contrast depends on bias, and thus also on the sharpness of the whole image, which is defined by the high slope of edges. Taking in account our experiments, we can claim that this only holds for less degraded input images. For other input images, the contrast is more dependent on enhancing the SNR than on preserving the steepness of edges.

The effect of the thresholding methods used can be characterized as follows: hard thresholding preserves the edge steepness of the input image and then the resultant contrast is higher. At the same time, SNR is not so high because of the discontinuities between cancelled and retained wavelet coefficients. On the other hand, soft thresholding thanks to fewer discontinuities among wavelet coefficients improves the SNR, but reduces the edge steepness (the image is more blurred),

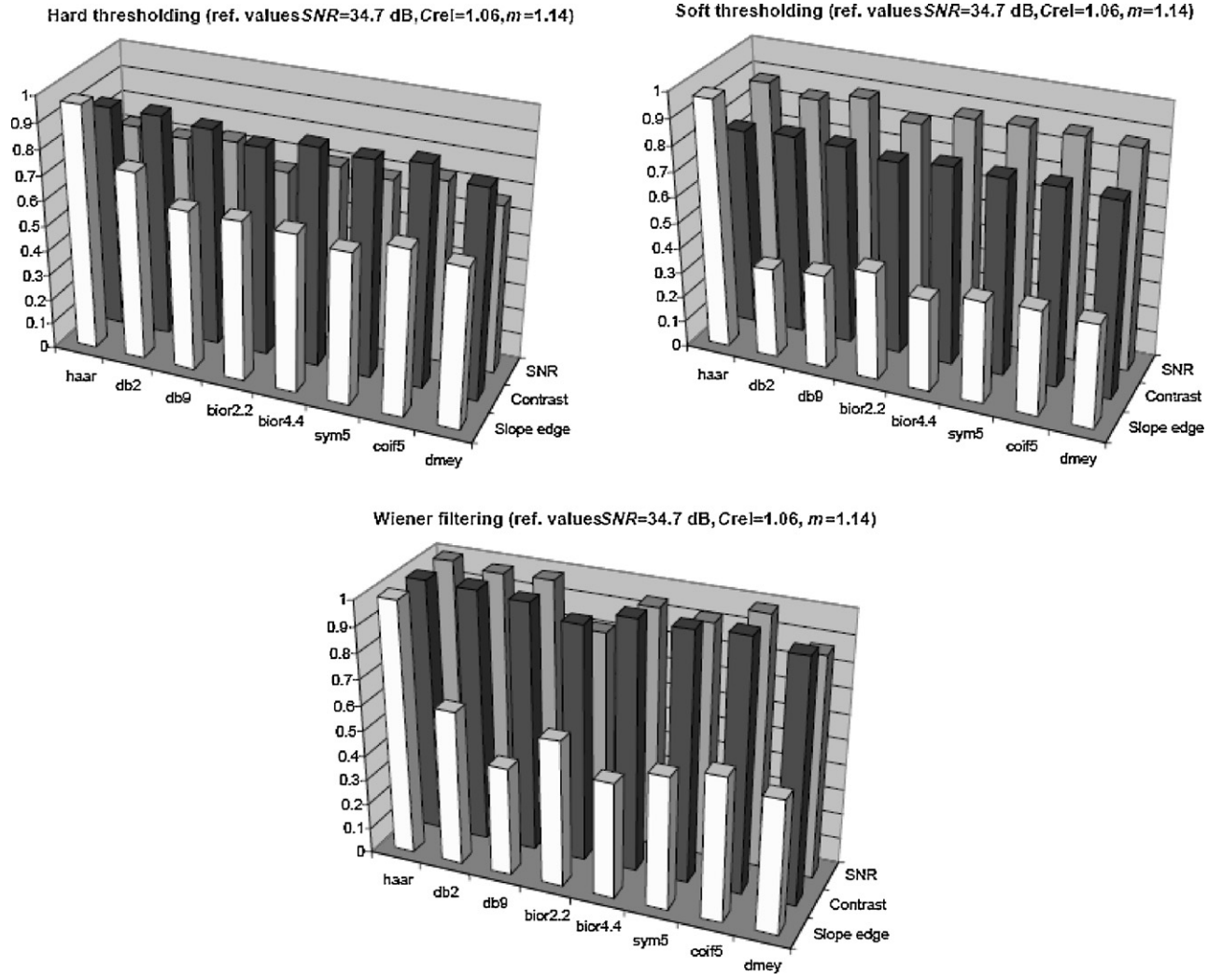

Fig. 5 – Results of de-noising the phantom MR image with SNR = 19.1 dB.

Table 3 – Results of de-noising the MR image of head with SNR = 33 dB.

Wavelet filter	Hard thresholding				Soft thresholding				Wiener filtering			
	SNR	C_{rel}	m_1	m_2	SNR	C_{rel}	m_1	m_2	SNR	C_{rel}	m_1	m_2
haar	47.1	0.97	0.99	0.94	50.7	0.97	0.87	0.35	49.8	0.97	0.95	0.79
db2	43.5	0.97	0.97	0.91	47.9	0.97	0.78	0.62	46.9	0.98	0.83	0.72
db9	42.3	0.97	0.98	0.97	49.0	0.97	0.79	0.60	47.4	0.97	0.82	0.86
bior2.2	38.8	0.97	0.98	0.97	46.6	0.97	0.96	0.79	44.4	0.97	1.00	0.91
bior4.4	42.6	0.97	0.97	0.88	49.5	0.97	0.81	0.77	48.4	0.97	0.84	0.87
sym5	43.9	0.97	0.86	0.93	49.8	0.97	0.83	0.59	48.7	0.97	0.86	0.86
coif5	42.7	0.97	0.97	0.73	48.8	0.97	0.80	0.58	47.7	0.97	0.84	0.67
dmey	41.2	0.97	0.98	0.96	48.4	0.97	0.85	0.80	47.1	0.97	0.88	0.90

and bias is inserted and results in less contrast. The Wiener filtering of the wavelet coefficients suppresses the disadvantages of the two above-mentioned thresholding methods, but only on condition that parameter τ is known a priori. Its value depends on the particular MR image. Therefore, the Wiener filtering is not useful for full automatic processes. It can be said that hard thresholding is useful for high SNR input images, soft thresholding is more convenient for low SNR input images, and, finally, the Wiener filtering is useful for all MR images, but only if an optimum parameter τ can be estimated in advance.

The choice of the mother wavelet (wavelet filter) greatly affects the resultant image quality. Eight different mother wavelets were taken into account in this paper. The Haar wavelet was the most useful for simple images (not many details) with high slope edges (sharp transitions), especially with hard thresholding. The greatest disadvantage of hard thresholding is the difficulty of obtaining smoothly reconstructed images, which is manifested by disturbing rectangular artifacts. Mother wavelets of the Daubechies type are typical representatives of non-symmetrical wavelets, which are used with both plain images and images with many details (so complicated) to obtain a higher SNR value (but less steep edges, of course). It is the reason why they are combined with soft thresholding. If the order of the Daubechies wavelets increases, then the slope steepness tends to decrease and, on the contrary, SNR becomes higher. Bi-orthogonal wavelets, which belong to symmetrical wavelets, yield a good balance between high slope edge and high SNR for all threshold methods. Consequently, they are optimal wavelets for much complicated images in order to obtain a good balance between SNR and image sharpness. Higher-order bi-orthogonal wavelets give outputs similar to wavelets of the Daubechies type. Wavelets of the Coiflet or Symlet type give identical results for plain images. They give a high SNR at the cost of lower slope edge. When the Coiflet and Symlet wavelets were applied to more complicated images, they differed in edge slope ratios m_1 and m_2 for hard thresholding. It can be said that they behave like the Daubechies wavelets. The discrete Meyer wavelets exhibit advantages that can, in particular, be seen when the Wiener filtering of wavelet coefficients is used for more complex images. A high degree of correspondence between SNR and the preservation of the steepness of the two image edges measured, m_1 and m_2, was obtained. A similar correspondence was obtained in the application of soft thresholding. The discrete Meyer wavelet is recommended to be used as a universal mother wavelet for processing complicated images in combination with soft thresholding.

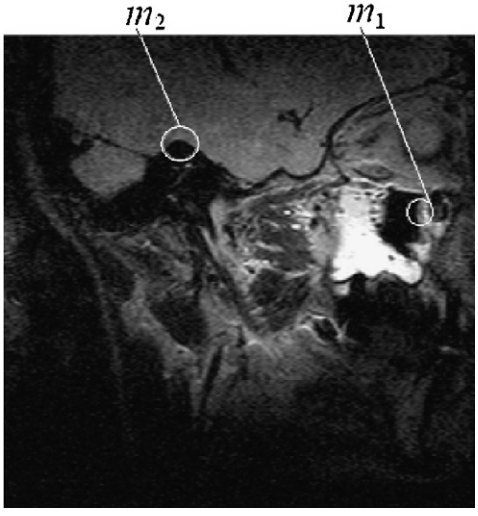

Fig. 6 – Test MR image of head with areas of slope edge measurement.

4.2. *A brief summary of how to select optimal parameters*

The choice of optimal parameters for noise suppression in MR images using the wavelet analysis can be divided into several steps depending on the image type:

(a) *Format*. It is recommended to process both the image magnitude and the image phase in order to suppress bias in the resultant image (while preserving a higher contrast). However, it is not always that the phase is available.
(b) *Quality*. It is recommended to use the hard thresholding for images with a high SNR ratio while the soft thresholding is preferably used for images of bad quality, which require a substantial increase of the SNR.
(c) *Structure*. The mother wavelets of the Haar or the Daubechies type should be used for images with a simple structure (for example, test image of phantom), the mother wavelets of the Mayer or the Symlet type should be used for images with a more complex structure (for example, test image of the head).
(d) *Fineness of resolution*. If preserving the highest possible degree of image detail is required, it is recommended to use the hard thresholding together with the discrete Mayer mother wavelet or the Daubechies mother wavelet of higher order.

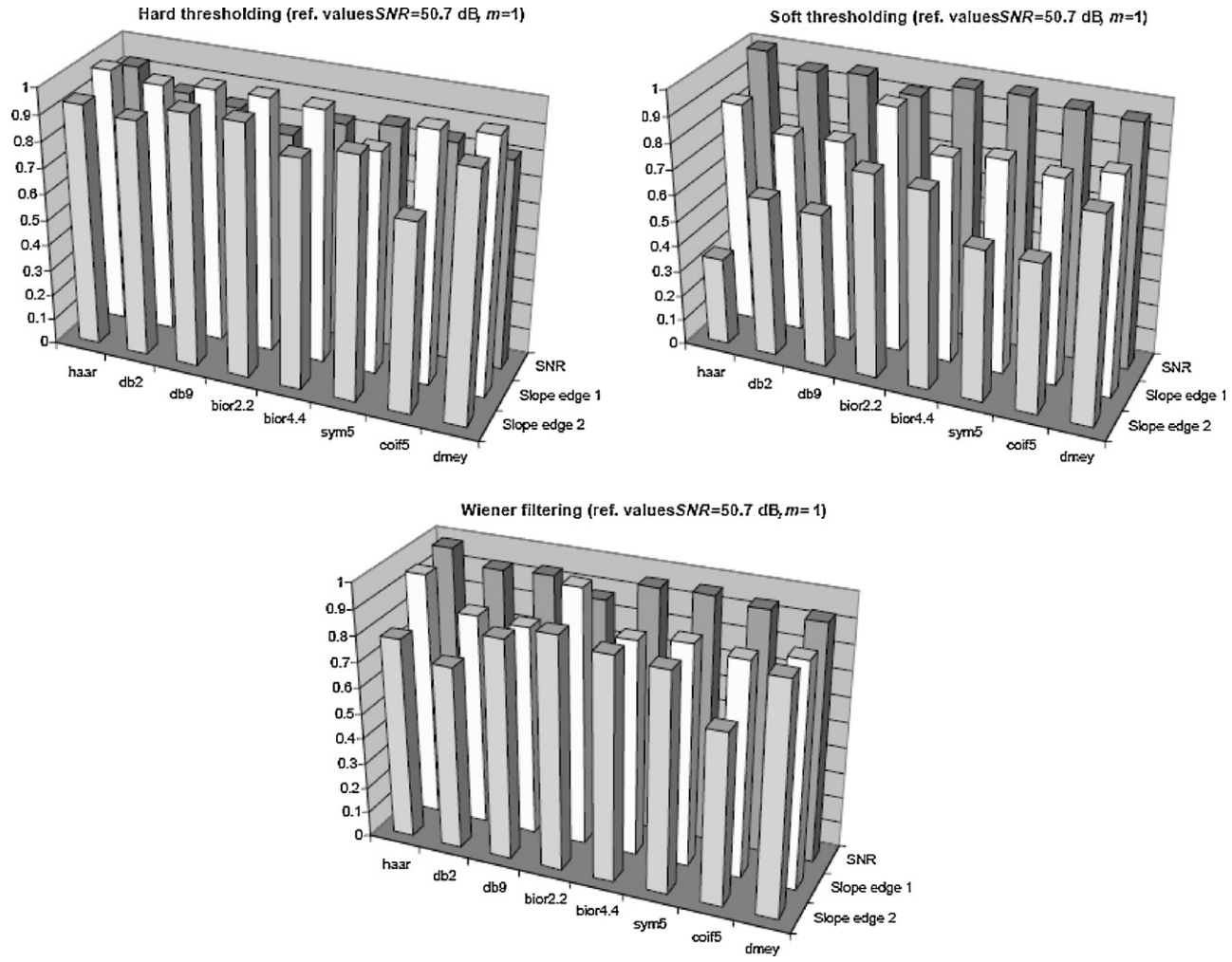

Fig. 7 – Results of de-noising the MR image of head with SNR = 33 dB.

(e) In the case of semi-automatic image enhancement, the Wiener filter should be used with optimal setting of parameter τ.

5. Conclusion

In this paper, an evaluation of the wavelet-based de-noising efficiency for various mother wavelets is described. The real and imaginary parts of the MR image are filtered separately and the evaluation of filtering efficiency is realized on the output complex MR image, using three parameters: SNR, image intensity contrast, and intensity gradient in chosen parts of the MR image. To determine the influence of the choice of mother wavelet in combination with various types of thresholding on the monitored parameters (SNR, image contrast, and edge steepness of the linear approximation) both phantom and real MR images with different SNR values were used. Based on the results achieved, individual combinations were evaluated and a recommendation was made for attenuating noise in various types of image, complemented with a brief summary of how to choose optimal parameters of wavelet analysis with the aim of attenuating noise in MR images.

Acknowledgements

The paper has been supported by the Czech Science Foundation under grant No. P102/11/0318 and by the Ministry of Education, Youth and Sports under grant KONTAKT ME10123 and project No. CZ.1.05/2.1.00/01.0017.

REFERENCES

[1] J.B. Weaver, Y. Xu, D.M. Healy, L.D. Cromwell, Filtering noise from images with wavelet transforms, Magnetic Resonance Medicine 21 (1991) 288–295.
[2] R.M. Henkelman, Measurement of signal intensity in the presence of noise in MR images, Medical Physics 12 (1985) 232–233.
[3] R.D. Nowak, Wavelet-based rician noise removal for magnetic resonance imaging, IEEE Transactions on Image Processing 8 (10) (1999) 1408–1419.
[4] M.E. Alexander, R. Baumgartner, A.R. Summers, C. Windischberger, M. Klarhoefer, E. Moser, R.L. Somorjai, A wavelet-based method for improving signal-to-noise ratio and contrast in MR images, Magnetic Resonance Imaging 18 (2000) 169–180.

[5] S. Zaroubi, G. Goelman, Complex de-noising of MR data via wavelet analysis: application to functional MRI, Magnetic Resonance Imaging 18 (2000) 59–68.
[6] H. Cruz-Enriquez, V.J. Lorenzo-Giorni, Wavelet-based methods for improving signal-to-noise ratio in phase images, Lecture Notes in Computer Science 3656 (2005) 247–254.
[7] P.S Addison, The Illustrated Wavelet Transform Handbook, Institute of Physics, 2002.
[8] B. Vidakovic, Statistical Modelling by Wavelets (Wiley Series in Probability and Statistics), John Wiley & Sons, New York, 1999.
[9] D.L. Donoho, De-noising by soft-thresholding, IEEE Transactions on Information Theory 41 (1995).
[10] H. Braunish, W. Baeian, J.A. Kong, Phase unwrapping of SAR interferograms after wavelet de-noising, IEEE Geoscience and Remote Sensing Symposium 2 (2000) 752–754.
[11] G. Sadashivapp, K.V.S. Ananda Babu, Wavelet filters for image compression. An analytical study, International Journal on Graphics, Vision and Image Processing 9 (2009).
[12] H.F. Cancino-de-Greiff, R. Ramos-Garcia, V.J. Lorenzo-Giorni, Signal de-noising in magnetic resonance spectroscopy using wavelet transforms, Concepts in Magnetic Resonance 14 (2002) 388–401.